THE EFFECT OF FERMENTED DEGLYCYRRHIZINATED LIQUORICE EXTRACT ON THE STRUCTURE OF THE RENAL CORTEX IN EXPERIMENTALLY INDUCED DIABETES MELLITUS IN RATS: HISTOPATHOLOGICAL STUDY

Ahmad Mohamed Ali Massoud[1], Faika Hassan El Ebiary[2], Nebal Gamal Abd Elwahab[2] and Dalia Alaa El-Din Aly El-Waseef[2]

[1]Department of Hepato-gastroenterology and Infectious Diseases, Faculty of Medicine, Al Azhar University, Cairo, Egypt.
[2]Department of Histology & Cell Biology, Faculty of Medicine, Ain-Shams University, Cairo, Egypt

Corresponding author:
Dalia Alaa El-Din Aly El-Waseef
Mobile: +2 01001243948
E-mail:
daliaalaaelwaseef@med.asu.edu.eg

Received: 29/04/2024
Accepted: 30/05/2024

Online ISSN: 2735-3540

ABSTRACT:

Background: *Diabetic nephropathy is a severe consequence of diabetes mellitus. Liquorice was fermented and deglycyrrhizinated to remove glycyrrhizin; and given the name "fermented deglycyrrhizinated liquorice extract" (FDGL).*

Aim of the Work: *To study the potential ameliorating role of FDGL on the structural changes in renal cortex of adult male albino rats with experimentally induced diabetes mellitus.*

Methods: *Rats were randomly divided into three equal groups (n=15 per group): Group I (control), group II (diabetic): induction of diabetes was done via streptozotocin injection, and group III (FDGL-treated): after confirmation of diabetes, rats were left untreated for two weeks and then received oral FDGL (0.12 g/kg body weight/day) for another two weeks before being sacrificed.*

Results: *The diabetic group showed some shrunken glomeruli surrounded by wide Bowman's spaces. Other glomeruli were enlarged. Proximal convoluted tubules (PCTs) appeared dilated with casts, their lining cells showed focal areas of lost apical brush border, and disruption of basement membrane. The interstitium showed extravasated blood, mononuclear cellular infiltration, and increased collagen fibers. Transmission Electron microscopy showed effacement of the podocytes` foot processes and thickening of the glomerular basement membrane. PCTs showed cytoplasmic vacuoles and disorganized mitochondria. Group III showed a histological structure of glomeruli and renal tubules comparable to that of the control group.*

Conclusion: *FDGL extract substantially ameliorated the adverse effects of diabetes on the structure of renal cortex in diabetic rats.*

Keywords: *Diabetes mellitus, Diabetic nephropathy, FDGL, Renal cortex, Rats, TEM.*

INTRODUCTION:

Diabetic nephropathy (DN) is one of the most dangerous and severe effects of diabetes mellitus (DM), which is linked to high rates of morbidity and death in patients with diabetes [(1).] Diabetes is becoming increasingly common, particularly in developing nations [(2)]. Inflammatory mediators, oxidative stress and angiotensin II are among the numerous mediators and pathways involved in the development of DN [(3&4)]. Oxidative stress is a condition in which an imbalance between oxidants and antioxidants results in oxidative damage to tissues [(5)]. Oxidative stress, including

hyperglycemia itself, is a common byproduct of numerous pathways implicated in DN pathogenesis [6]. The levels of IL-6, IL-18, TNF, TGF-β1 and other inflammatory mediators are raised in blood and showed a role in the development of DN [7].

Glycyrrhiza, or liquorice, has been used for more than 2,000 years and is considered the most widely prescribed natural medicine in China. Approximately thirty species make up the genus Glycyrrhiza [8]. The People's Republic of China Pharmacopeia lists G. inflate, G. uralensis, and G. glabra as liquorice's ancestors [9]. Liquorice flavonoids have notable antidiabetic potential. Ethanol extract of G. glabra can reduce the symptoms of diabetic nephropathy and chronic hyperglycemia; additionally, in obese and diabetic rats, the liver microsomal diacylglycerol acyltransferase activity was inhibited by the ethanol extract of G. uralensis, while G. inflate effectively prevented DN, vascular complications related to diabetes, and endothelial dysfunction [10]. Liquorice ethanol extracts and flavonoid oil showed hypoglycemic and abdominal lipid-lowering effects in obese diabetic KK-Ay mice [11]. Moreover, liquorice flavonoid oil has been demonstrated to have therapeutic effects on DM and hyperglycemia in KK-Ay mice by regulating glucose metabolism via the AMPK pathway [12].

In the West, people have been using liquorice since the times of the ancient Egyptians, Greeks, and Romans [13]. Products made from liquorice are most frequently used as food additives [14]. One of the main phenolic components of liquorice species, licochalcone A, along with Glycyrrhizae Radix, provides protection against protein glycation reactions [15]. Liquorice has been shown in several studies to alleviate glucose intolerance and enhance insulin sensitivity [16]. According to *Yang et al.* [17], liquorice inhibits free radical damage, insulin resistance, and oxidative stress, all of which significantly slow the progression of diabetes. However, consuming too much liquorice can cause muscle weakness, hypertension, and potassium loss. This is due to glycyrrhizin that is present in liquorice. Glycyrrhizin causes water and sodium retention and elevates blood pressure. Due to the potential for hypertensive side effects from glycyrrhetinic acid in liquorice, deglycyrrhizinated liquorice extract (DGL) is most often used [18].

Alpha amylase, one of the enzymes produced during the fermentation of liquorice, is essential for reducing the complications associated with diabetes. The substance that gives liquorice its various adverse effects, glycyrrhizin, was then eliminated by deglycyrrhizinating the liquorice. According to *Massoud* [19], this medication is therefore known as fermented deglycyrrhizinated liquorice extract (FDGL). According to several studies, liquorice may have antidiabetic effects by promoting the activation of "peroxisome proliferator activated receptor gamma (PPARγ)"; this process is involved in the metabolism of lipid and carbohydrate as well as adipocyte differentiation [20]. Additionally, glabridin increases the amount of glucose consumed and prevents glucose intolerance by enhancing the translocation of glucose transporter type 4 through adenosine monophosphate protein kinase [21].

AIM OF THE WORK:

The purpose of the current study was to assess the possible ameliorating effect of FDGL extract on the structural changes of the renal cortex in a rat model of diabetes mellitus.

MATERIALS AND METHODS:

The experimental procedures were performed at the Medical Research Center, in the Faculty of Medicine, A.S.U., Cairo, Egypt.

Animals:

In this study, 45 adult male albino rats in good health; with ages ranging from two to three months, and average weights between 180 and 250 g were utilized. The animals were kept in healthy, well-ventilated rooms with appropriate lighting, temperature, and humidity. The rats, housed in stainless steel cages with mesh wire covers, had unrestricted access to food and water. Animal procedures were performed in compliance with the National Institute of Health guide for the use and care of Laboratory animals (NIH Publications No. 8023, revised 1978) and according to the guidelines of Animal Care.

Drug preparation:

Based on the EUROPEAN PATENT SPECIFICATION Ep 1 925 312 B1, fermented deglycyrrhizinated liquorice (FDGL) extract powder was made by three sequential steps: lyophilization, deglycyrrhizination, and fermentation of liquorice roots [(19)]. Both, the acute toxicity of FDGL extract [(22)], and the chronic toxicity [(23)] were assessed in adult rats in an earlier stage of the study, performed in the Pharmacology Research Unit, National Research Center, Cairo, Egypt. It was found that it is safe to use oral FDGL extract up to 0.12 g/ kg body weight daily for two months.

Induction of DM by STZ

The rats were confirmed to be normoglycemic at the start of the experiment by measuring their blood glucose levels. After a fasting period of 18-hour, the selected rats received streptozotocin (STZ) injection to induce diabetes mellitus. Freshly prepared solution of STZ (Sigma, Aldrich, USA) was injected once, intraperitoneally at a dose of 45 mg/kg body weight diluted in 0.5 mL of 0.1 M/L citrate buffer with pH 4.5. Three days later, One Touch Ultra 2 glucose meter and strips (LifeScan, Inc. USA) were used to assess the fasting blood glucose (FBG) from the tail vein [(24&25)]. Rats were classified as diabetics and selected for the study when having a fasting blood glucose level (FBG) of 250 mg/dL or higher [(26)].

Animal Grouping

Animals were allowed to acclimatize for seven days, then they were randomly divided into three equal groups, (n=15 per group).

Group I (Control):

Was further subdivided into three equal subgroups (n=5).

- **Subgroup Ia:** No intervention. Rats were sacrificed after four weeks.
- **Subgroup Ib:** Each rat received one injection of 0.5 mL of 0.1 M/L citrate buffer intraperitonially as a vehicle of STZ. Rats were sacrificed after four weeks.
- **Subgroup Ic:** As subgroup Ib. Rats were left without treatment for two weeks, then every rat was given freshly prepared FDGL extract orally for an additional two weeks at a dose of 0.12 g/kg body weight/day, dissolved in 2 mL of distilled water [(27)].

Group II (Diabetic):

Induction of diabetes was done in rats of this group. After being confirmed as diabetics, rats were left without further intervention for four weeks and then were sacrificed.

Group III (Diabetic treated with FDGL extract):

Induction of diabetes was done in rats of this group as in group II. After being confirmed as diabetics, rats were left without treatment for two weeks. Then they received oral FDGL extract daily for further two weeks as in subgroup Ic and then were sacrificed.

Measurement of Fasting Blood glucose (FBG):

One Touch Ultra 2 glucose meter and strips (LifeScan, Inc. USA), were used to measure (FBG) levels twice weekly for each

animal, during fasting, by taking a fresh drop of blood from the tail vein. Data was collected and subjected to statistical analysis.

Preparation of samples for Histological study:

The animals were sacrificed by decapitation under the effect of ether inhalation anesthesia. For light microscopic (LM) study, the right kidneys were extracted and fixed in 10% formalin. Followed by dehydration, clearing, then finally embedding in paraffin. Serial sections of 5µm thickness were cut and stained with Hematoxylin and Eosin (H&E) stain, Periodic acid Schiff (PAS) and Mallory`s trichrome stain [28]. For transmission electron microscopic (TEM) study, the left kidneys were extracted. Small parts (1 mm^3) of the cortex were cut. The tissues were immediately fixed in 2.5% phosphate buffered glutaraldehyde followed by 1% osmium tetroxide, dehydrated, and embedded in epoxy resin. Semithin sections (0.5-1 µm) were stained with 1% toluidine blue and examined by LM for orientation [28]. Ultrathin sections (80 nm) were examined and photographed by TEM [JEOL- 1010 made in Japan] at the EM Unit, in the Faculty of Science, A.S.U., Cairo, Egypt.

Histo-morphometric study and statistical analysis

A morphometric study was conducted on five animals per group. Five distinct slides from each animal were used for measurements. For every slide, five high-power, non-overlapping fields at a magnification of ×400 were chosen at random and examined. Each sample was photographed five times, and the mean value for each specimen was determined. An impartial observer who was blinded to the specifics of the specimens took measurements to make an assessment.

Measurements were obtained using a Leica DM2500 microscope (Wetzlar, Germany) connected to a computer running the Leica Q-Win V.3 image analyzer software, at the Histology Department, Faculty of Medicine, A.S.U.

Data were analyzed, and then, subjected to statistical study though post-Hoc test at least significant difference (LSD) and one-way analysis of variance (ANOVA) using the SPSS.21 program (IBM Inc., Chicago, Illinois, USA). P-values were determined as significant if they were less than 0.05 and as non-significant if they were greater than 0.05. The data summary is presented as the mean ±SD (standard deviation).

The measured parameters include:

1. Width (µm) of Bowman's spaces in the glomeruli of the different groups.
2. Area percentage (%) of collagen fibers in the renal cortex of the different groups.

Ethical Considerations:

Research Ethical Committee of Faculty of Medicine, Ain Shams University (FMASU REC) which is organized and operates according to guidelines of the International Council on Harmonization (ICH) and the Islamic Organization for Medical Sciences (IOMS), the United States Office of Human Research Protections and the United States Code of Federal Regulations, and operates under the Federal Wide Assurance number FWA 000017585, while the research approval number is (FMASU R275/2023).

RESULTS:

The diabetic group (group II) recorded the death of 3 rats.

Histological examination of the kidney specimens:

All subgroups of group I (Control) showed almost similar histological pictures in LM and TEM, so they will all be described as (control group).

A. Light microscopic examination:

1. H&E:

Examination of control sections revealed that the renal cortex was composed of renal glomeruli, and proximal and distal convoluted tubules. Each glomerulus consisted of glomerular tuft of capillaries surrounded by a narrow Bowman's space. The proximal convoluted tubules (PCTs) had narrow lumina and were lined by pyramidal cells with indistinct boundaries. They had deep acidophilic cytoplasm, and basal rounded vesicular nuclei. The distal convoluted tubules (DCTs) had wide lumina and were lined by cubical cells containing acidophilic cytoplasm and central rounded nuclei (Figure 1 (A, B, C)).

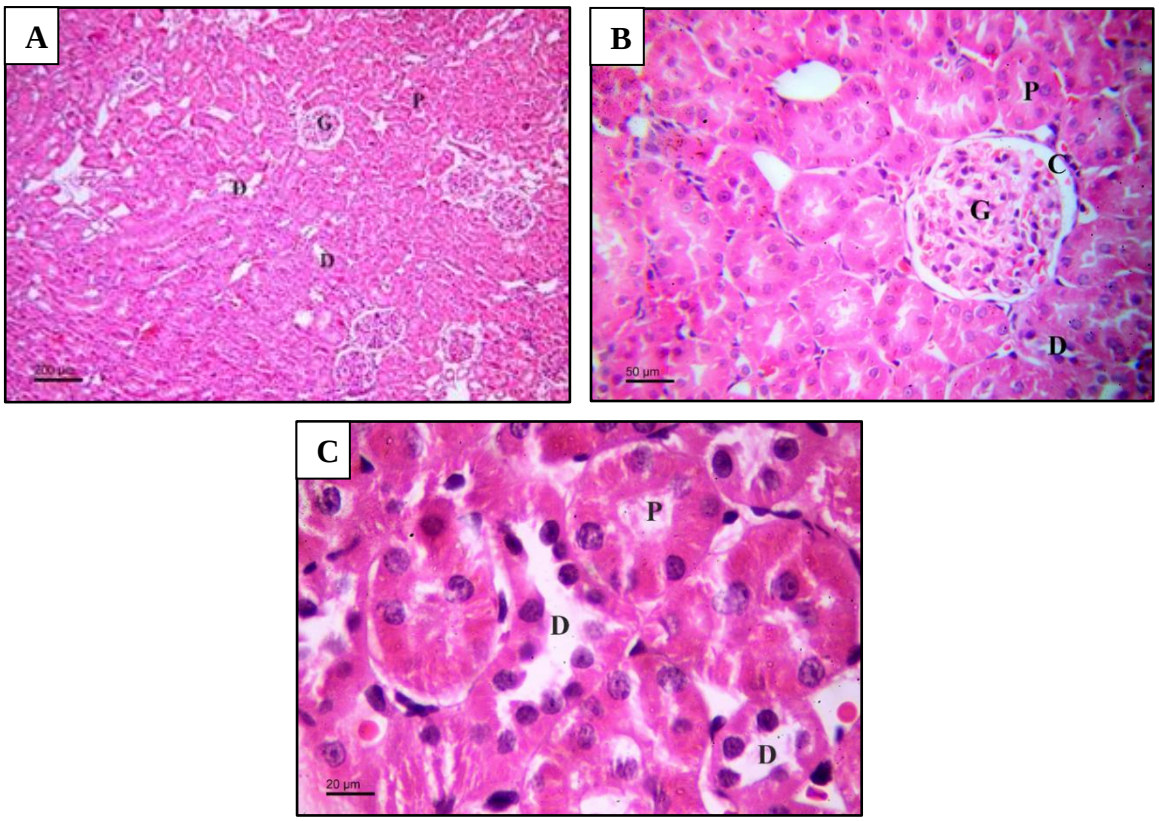

Figure 1 (A, B, C): Showing the renal cortex of rats of **group I (control)**. **A:** renal glomeruli (G) are surrounded by Bowman's capsules, the PCTs (P), and the DCTs (D). **B:** showing a renal glomerulus (G) surrounded by narrow capsular space (C). PCTs (P) are lined by pyramidal cells with indistinct boundaries, acidophilic cytoplasm, and basal rounded vesicular nuclei. DCTs (D) appear lined by cubical cells with acidophilic cytoplasm and central rounded nuclei. **C:** showing PCTs (P) lined by pyramidal cells with indistinct boundaries, acidophilic cytoplasm, and basal rounded vesicular nuclei. DCTs (D) are lined by cubical cells with acidophilic cytoplasm and central rounded nuclei. [Group I, H&E: **A** ×100, **B** ×400, **C** ×1000]

Glomeruli in group II (diabetic group) were substantially shrunken, with an apparent widening of the Bowman's spaces (Figure 2 (A&B)). Some glomeruli appeared enlarged (glomerular hypertrophy) and their mesangia showed apparently increased number of cells (apparent mesangial proliferation) Figure (2C). Some tubules appeared dilated, and their cells had pyknotic nuclei. Other cells had deep homogenous acidophilic cytoplasm. Some renal tubules showed extruded cells within their lumina, while other cells showed vacuolated cytoplasm. Homogenous acidophilic material was observed within the lumina of some PCTs. The renal interstitium showed focal extravasation of blood elements and mononuclear cellular infiltration (Figure 2(C,D,E,F)).

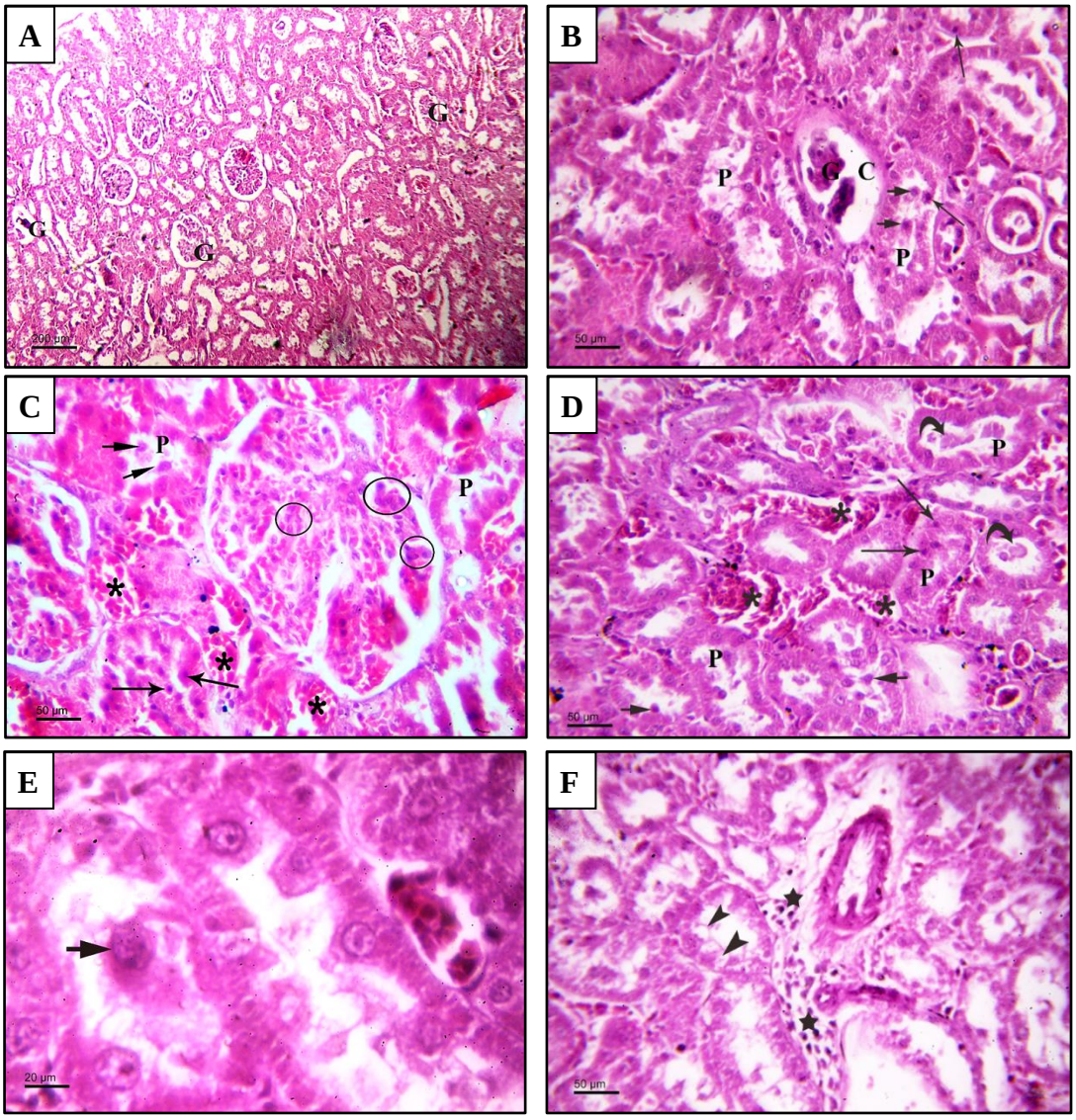

Figure 2 (A - F): Showing the renal cortex of rats from **diabetic group**. **A:** showing many shrunken glomeruli (G) with apparent widening of the capsular spaces. **B:** showing a shrunken glomerulus with apparent dilation of Bowman's space (C). Some tubules appear dilated (P) with extruded cells in their lumina (short arrow). Some cells lining the tubules have pyknotic nuclei (↑). **C:** showing an enlarged glomerulus (glomerular hypertrophy) with apparently increased number of mesangial cells (Black rings). Some tubules appear dilated (P) with extruded cells in their lumina (short arrow). Some cells lining the tubules have pyknotic nuclei (↑). Notice the extravasated blood elements (*) in the interstitium. **D:** showing apparent dilated tubules (P). Some cells lining the tubules contain pyknotic nuclei (↑). Some tubules show homogenous acidophilic material (curved arrow), and others show extruded cells (short arrow) within their lumina. Notice the extravasated blood elements (*) in the interstitium. **E:** showing an extruded cell within the lumen of a renal tubule (short arrow). **F:** showing mononuclear cellular infiltration in the interstitium (star). Notice the vacuolated cytoplasm of the cells lining some tubules (arrowhead). [Group II: H&E: **A** ×100, **B, C, D, F** ×400, **E** ×1000]

Renal cortex of group III (treated group) was comparable to the control group. Most of the renal glomeruli had relatively narrow Bowman's spaces. A few scattered tubules appeared dilatated Figure (3A), and a few tubules showed vacuolated cytoplasm of their lining cells Figure (3B). Neither extravasated blood, nor mononuclear cellular infiltration were detected in the renal interstitium.

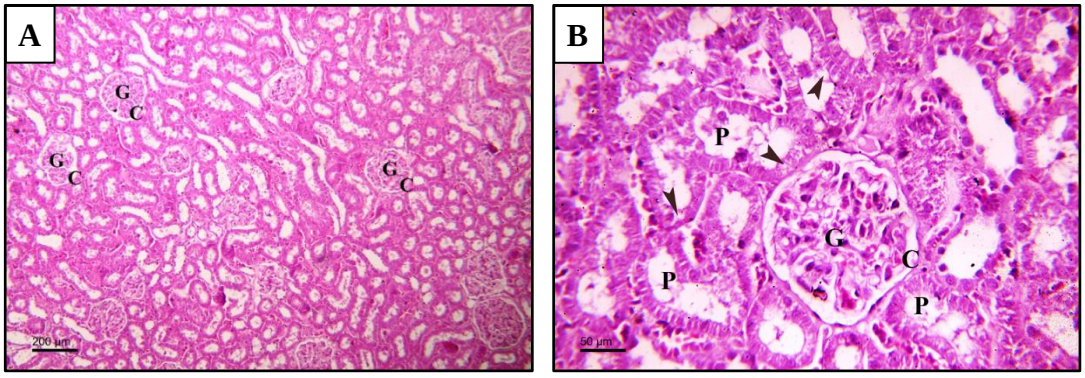

Figure 3 (A, B): Showing the renal cortex of rats of **group III (FDGL-treated group). A:** showing renal glomeruli (G) with narrow capsular spaces (C). Notice slight dilatation of some tubules. **B:** showing a renal glomerulus (G) surrounded by a narrow capsular space (C). Few PCTs show vacuolations (arrowhead) in the cytoplasm of their lining cells. Notice slight dilatation of some tubules (P).

[Group III, H&E: **A** ×100, **B** ×400]

2. Mallory's trichrome stain:

Examination of control sections revealed few thin collagen fibers around the renal corpuscles and tubules Figure (4A). The diabetic group showed apparently increased amount of collagen fibers around the renal corpuscles, tubules, and in the interstitium (Figure 4 (B & C)). Group III (treated group) showed thin collagen fibers comparable to those of the control group Figure (4D).

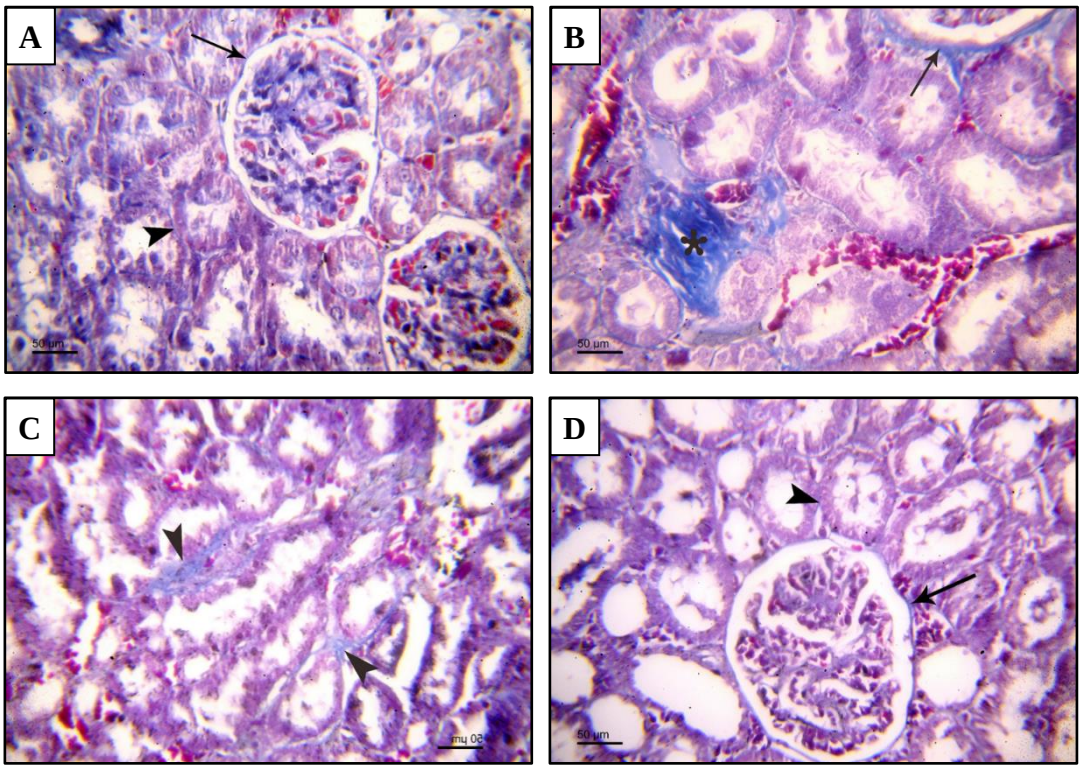

Figure 4 (A-D): Showing the renal cortex of rats. **A: control group:** few thin collagen fibers around the renal corpuscles (arrow) and the renal tubules (arrowhead). **B, C: diabetic group. B:** an apparent increase in collagen fibers around the renal corpuscle (arrow) and in the interstitium (*). **C:** apparent increase in collagen fibers around the renal tubules (arrowhead). **D: FDGL-treated group:** thin collagen fibers around the renal corpuscle (arrow) and the renal tubules (head arrow). [Mallory's Trichrome stain: **A-D** ×400]

3.PAS-stained sections:

The control group showed apical PAS-positive brush borders on the PCTs' cells. The surrounding basement membrane of the renal corpuscle, the renal tubules, and the glomerular blood capillaries showed a well-defined PAS-positive reaction Figure (5A). In the diabetic group, localized loss of the apical brush border was noticed in some PCTs cells. The basement membrane surrounding the renal corpuscle, the glomerular capillaries, and most of the renal tubules showed a well-defined PAS-positive reaction. The basement membrane of some renal tubules appeared disrupted Figure (5B). Several renal corpuscles showed glomerular hypertrophy and an apparent increase in the number of mesangial cells Figure (5C). Other renal corpuscles showed shrunken glomeruli and thick BM in the parietal layer of Bowman's capsule Figure (5D). Some tubules had a thick basement membrane, and their lining cells were pale with ill-defined boundaries (focal tubular atrophy). The interstitium showed many inflammatory cells (interstitial inflammation) Figure (5E). Group III (treated group) had PAS-positive apical brush borders of most PCTs cells. The basement membrane surrounding the renal corpuscle, renal tubules and glomerular capillaries showed a well-defined PAS-positive reaction Figure (5F).

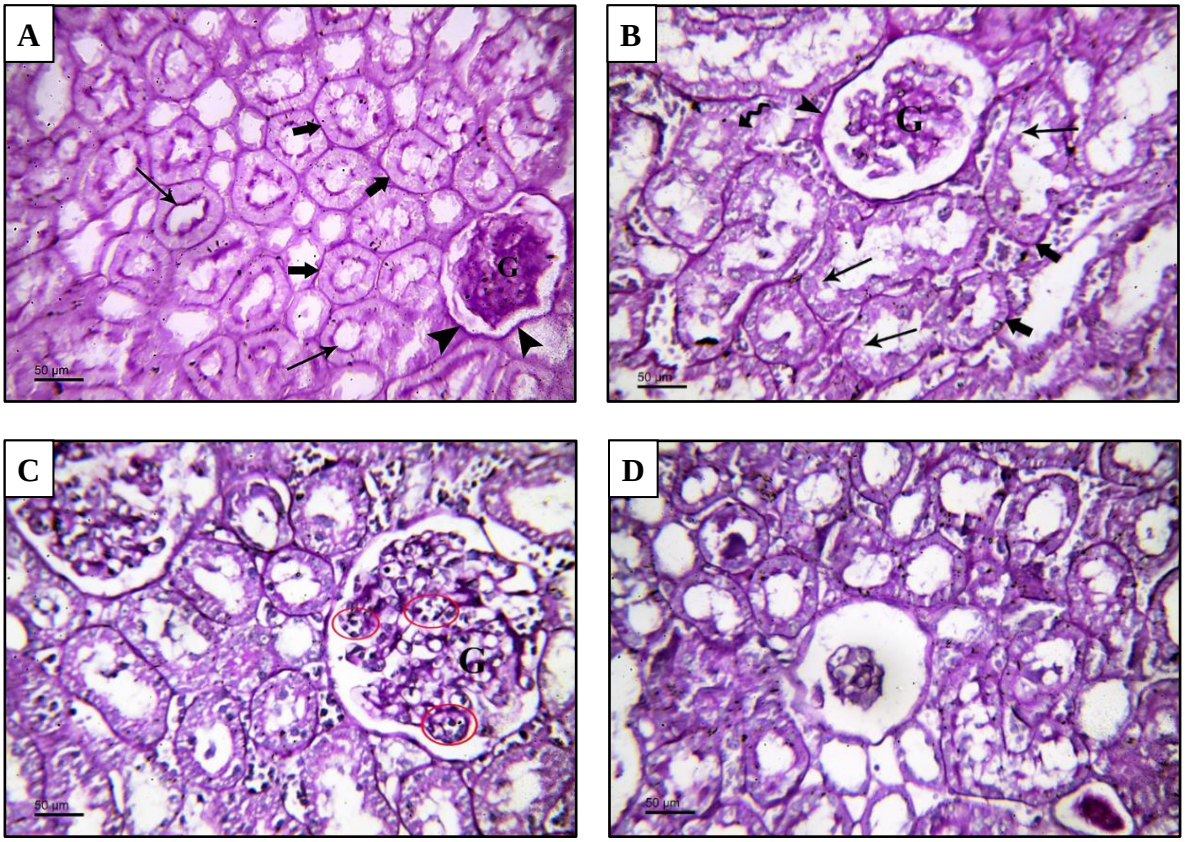

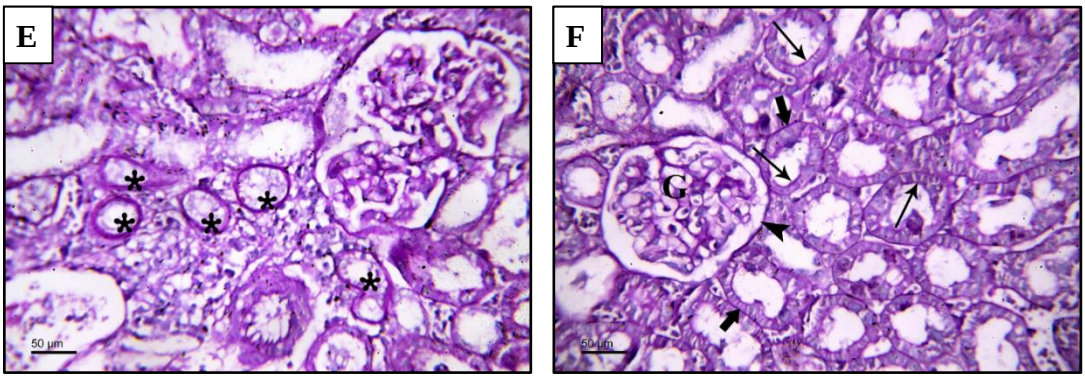

Figure 5 (A-F): Showing the renal cortex of rats. **A: control group:** apical PAS-positive brush borders of the cells of the PCTs (↑). The surrounding basement membrane of the renal corpuscle (▲), the renal tubules (thick arrow) and the glomerular blood capillaries (G) shows a well-defined PAS positive reaction. **B-E: diabetic group. B:** focal loss of the apical brush border in the cells of some PCTs (↑). The basement membrane surrounding the renal corpuscle (▲), the glomerular capillaries (G) and most of the renal tubules (thick arrow) shows a well-defined PAS positive reaction. The basement membrane of some renal tubules appears disrupted (wavy arrow). **C:** Some renal corpuscles show glomerular hypertrophy (G) and apparently increased number of mesangial cells (red rings). **D:** showing glomerular atrophy, thick BM of the parietal layer of Bowman's capsule. **E:** Notice several tubules (*) have thick basement membrane, and their lining cells are pale with ill-defined boundaries. The interstitium show many inflammatory cells (interstitial inflammation). **F: FDGL-treated group** showing PAS positive apical brush border of the most cells lining the PCTs (↑). The basement membrane surrounding the renal corpuscle (▲), renal tubules (thick arrow) as well as the glomerular capillaries (G) shows a well-defined PAS positive reaction. [PAS-stain: **A-E** ×400]

B. Transmission Electron Microscopic Examination:

Examination of ultrathin sections from the control group, revealed podocytes with primary processes arising from their cell bodies. Secondary processes (foot processes) appeared to project from the primary processes, and rest on the glomerular basement membrane. The glomerular basement membrane was seen thin and uniform in diameter. Filtration slits appeared between the podocytes` foot processes. The endothelium of the glomerular blood capillaries appeared fenestrated Figure (6). The PCTs were surrounded by a thin regular basement membrane. They were lined by pyramidal cells with central rounded euchromatic nuclei, basal elongated mitochondria, lysosomes, and long apical microvilli. Figure (7). The DCTs were surrounded by a thin regular basement membrane. They were lined by cubical cells with euchromatic nuclei, basal infoldings, elongated mitochondria and few short apical microvilli. Figure (8).

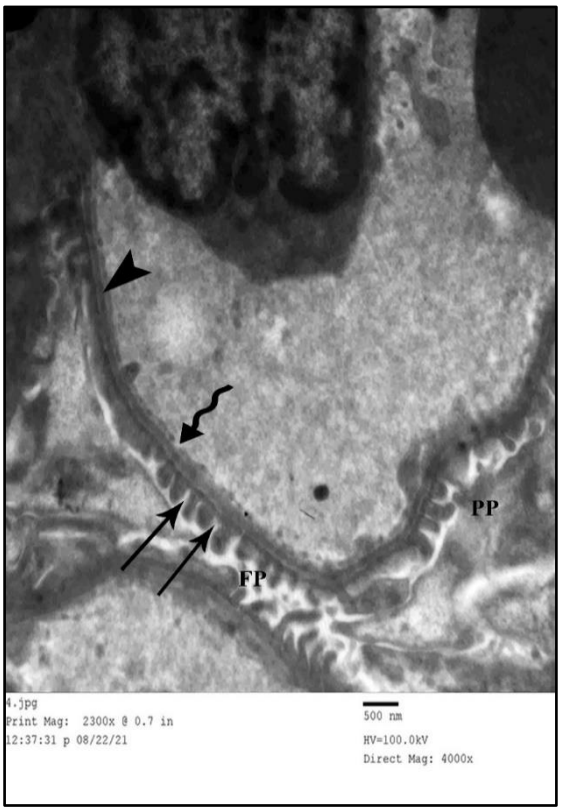

Figure 6: TEM image of the renal cortex from **group I (control group),** showing a podocyte with primary processes arising from its cell body. Foot processes (FP) appear to project from the primary processes (PP) and rest on the glomerular basement membrane. The glomerular basement membrane (arrowhead) is thin and regular in diameter. Filtration slits (↑) appear between the podocyte`s foot processes. The endothelium of the glomerular blood capillaries appears fenestrated (wavy arrow).(Group I. TEM. × 4000).

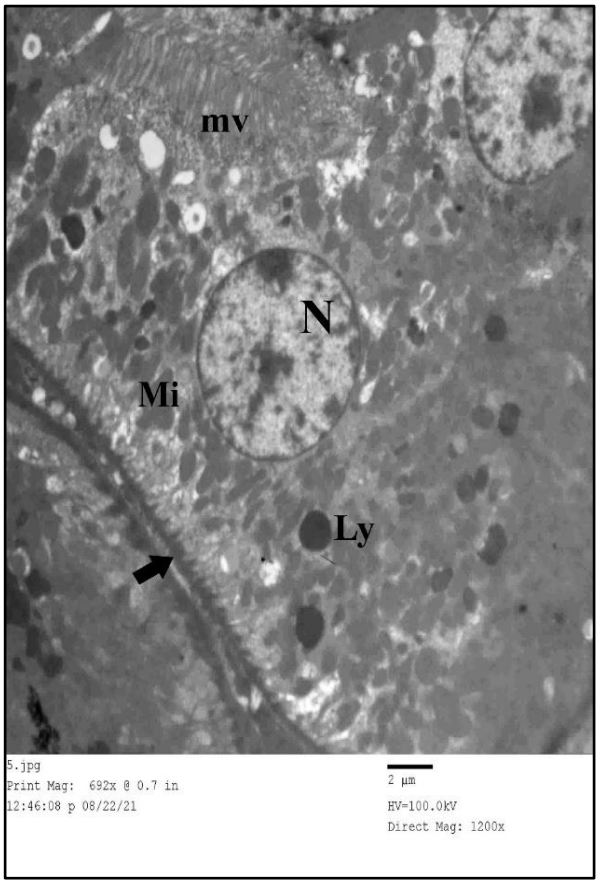

Figure 7: TEM image of the renal cortex from **group I (control group)** showing a portion of the PCT; their lining cells show euchromatic central rounded nuclei (N) and elongated basal mitochondria (Mi). Luminal borders show long microvilli (mv). Thin regular basement membrane (short arrow) and lysosomes (Ly) can be observed.

(Group I, TEM × 1200)

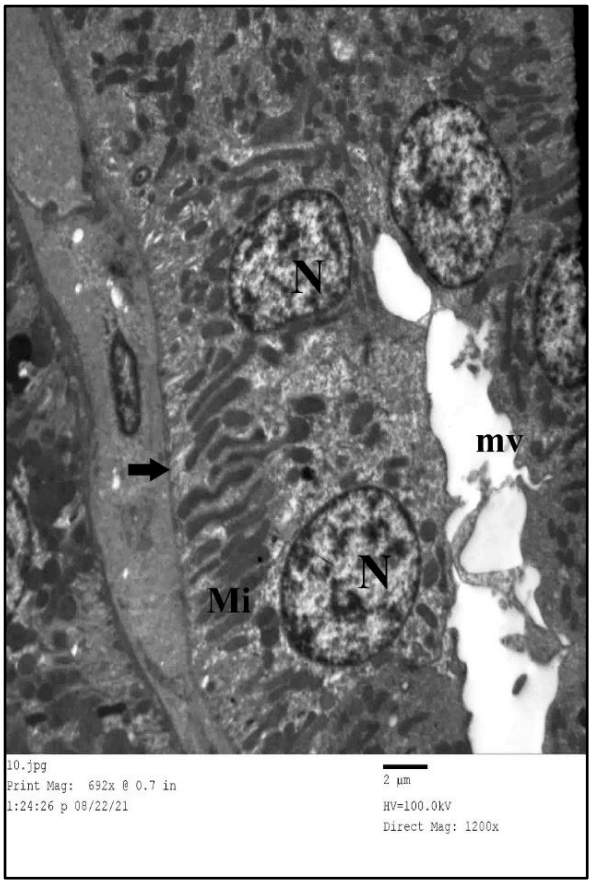

Figure 8: TEM image of the renal cortex from **group I (control group)** showing part of the DCT; their lining cells show few short apical microvilli (mv). Notice basal infoldings and elongated mitochondria (Mi); thin basement membrane (short arrow) and euchromatic nuclei (N) are also observed.

(Group I, TEM × 1200).

The glomerular basement membrane in the diabetic group was relatively thickened and irregular with effacement and derangement of the podocyte's foot processes Figure (9). The PCTs were surrounded with thick basement membrane. Their lining cells showed loss of basal infoldings and an irregular distribution of mitochondria Figures (10&11). Other cells of PCTs showed cytoplasmic vacuoles, and rarified cytoplasm (Figure 11). The DCTs showed some degenerated cells. The degenerated cells had small heterochromatic nuclei, rarified cytoplasm Figure (12) and disrupted basal infoldings with irregular distribution of mitochondria Figures (13&14).

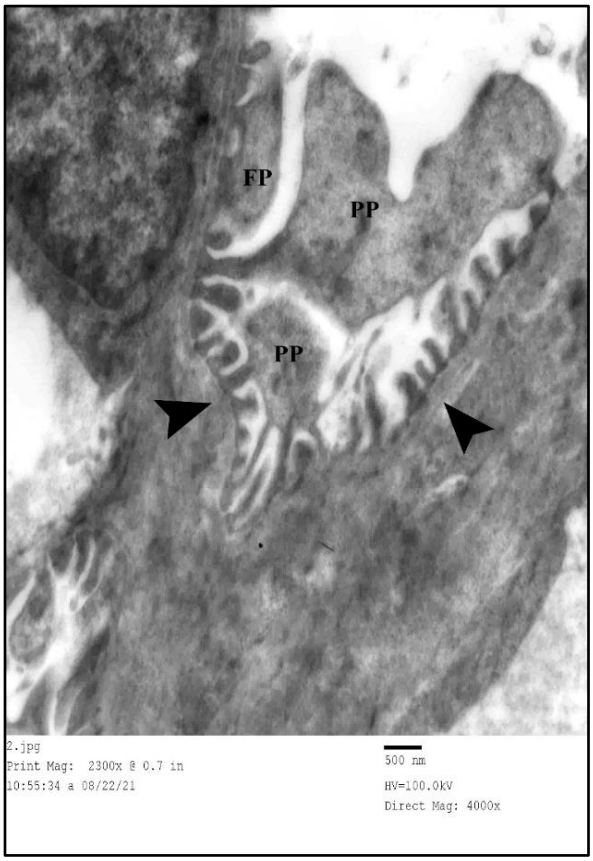

Figure 9:

TEM image of the renal cortex from **group II (diabetic group),** showing thick and irregular glomerular basement membrane (arrowhead). The foot processes (FP) are disarranged and show effacement. PP: 1ry processes of podocytes.

(Group II, TEM, × 4000).

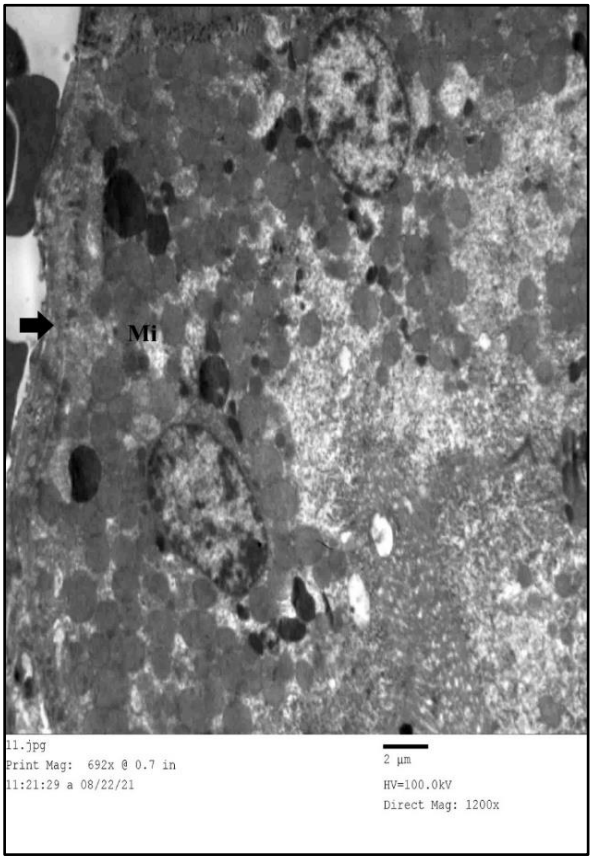

Figure 10:

TEM image of the renal cortex from **group II (diabetic group),** showing part of a PCT with a thick basement membrane (short arrow), loss of basal infoldings and irregular distribution of mitochondria (Mi).

(Group II, TEM, × 1200).

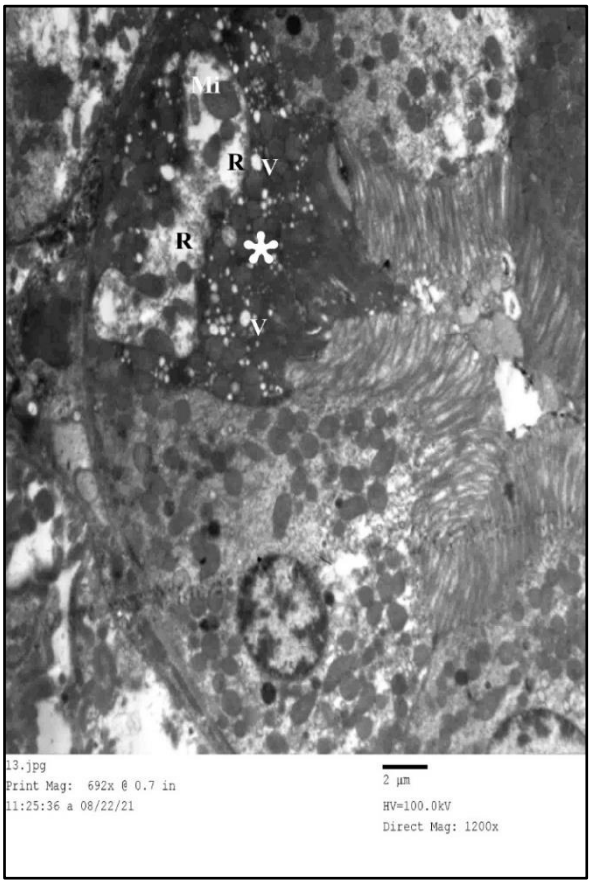

Figure 11:

TEM image of the renal cortex from **group II (diabetic group),** showing part of a PCT with a degenerated cell (*). The degenerated cell shows loss of basal infoldings and irregular distribution of their related mitochondria (Mi). Notice, cytoplasmic vacuoles (V), and rarified cytoplasm (R).

(Group II, TEM x1200 & × 3000).

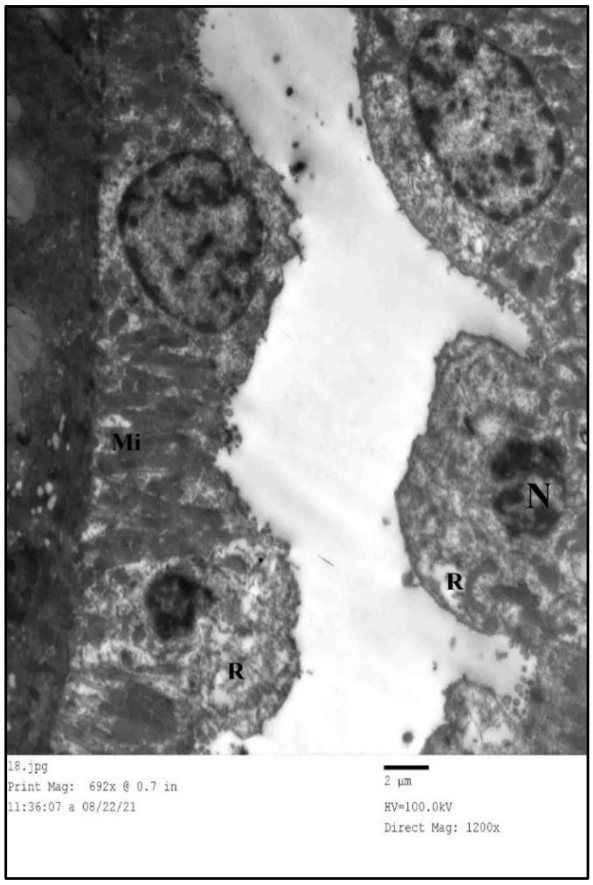

Figure 12:

TEM image of the renal cortex from **group II (diabetic group),** showing part of a DCT with some degenerated cells. The degenerated cells showing small irregular heterochromatic nucleus (N), rarified cytoplasm (R) and basal infoldings with elongated mitochondria (Mi).

(Group II, TEM × 1200).

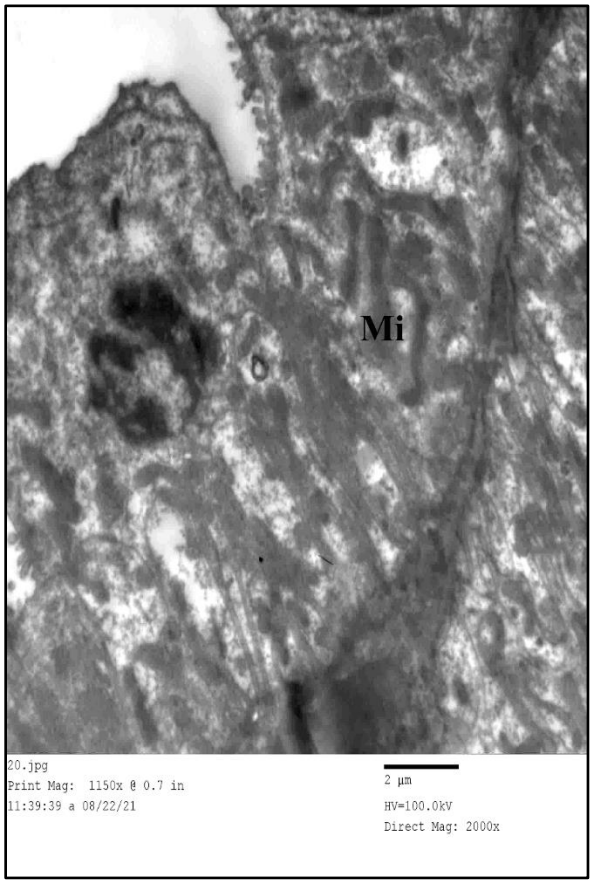

Figure 13:

TEM image of the renal cortex from **group II (diabetic group),** showing part of a DCT showing disruption of basal infoldings with abnormal distribution of mitochondria (Mi).

(Group II, TEM × 2000).

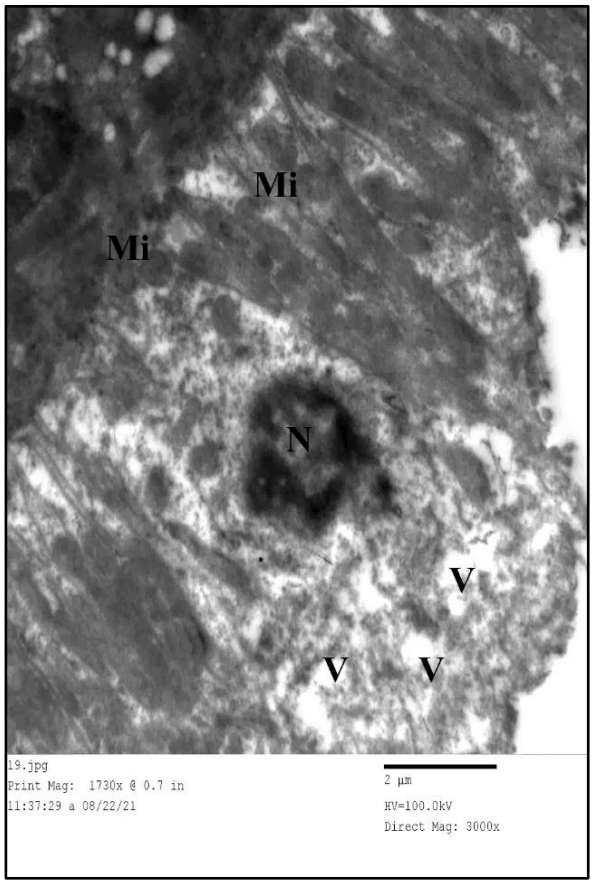

Figure 14:

TEM image of the renal cortex from **group II (diabetic group),** showing a portion of the DCT showing a small heterochromatic nucleus (N), disruption of basal infoldings with abnormal distribution of mitochondria (Mi). Notice the presence of cytoplasmic vacuoles (V).

(Group II, TEM × 3000).

Group III (treated group) exhibited a uniform thickness of the glomerular basement membrane. The foot processes of podocytes rested on the glomerular basement membrane. Filtration slits appeared between the podocyte's foot processes Figure (15). The PCTs were surrounded by a relatively thin basement membrane. They were lined by pyramidal cells with rounded euchromatic nuclei, basal elongated mitochondria and basal infoldings. They also contained lysosomes, endocytotic vesicles in their apical cytoplasm and long apical microvilli Figure (16). The DCTs were surrounded by a relatively thin basement membrane. They were lined by cubical cells with oval euchromatic nuclei, basal infoldings, elongated basal mitochondria and few short apical microvilli Figure (17).

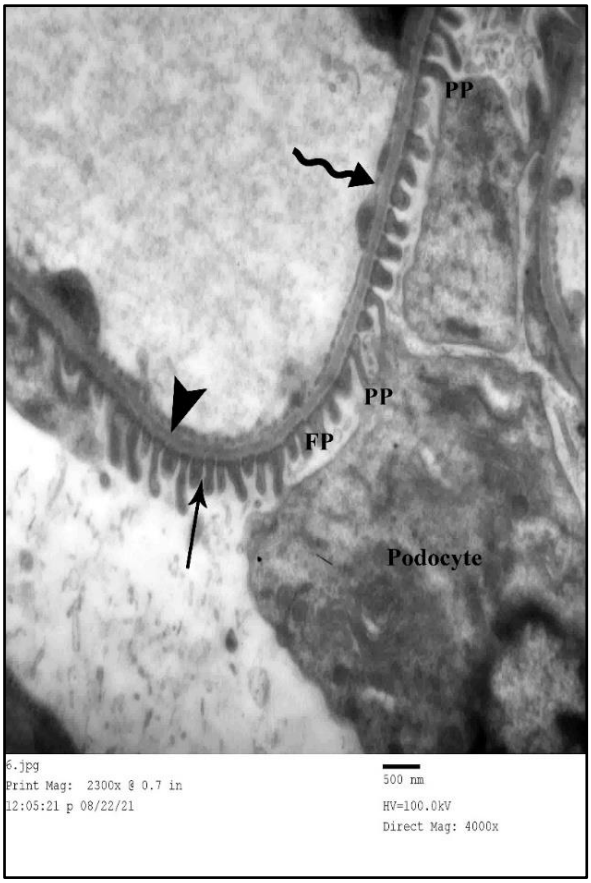

Figure 15:

TEM image of the renal cortex from **group III (treated group),** showing a glomerular basement membrane (arrowhead) with uniform thickness. The primary processes (PP) of podocytes arise from their cell body and the foot processes (FP) rest on the glomerular basement membrane. Notice, filtration slits (↑) appear between the foot processes of the podocyte. The endothelium of the glomerular blood capillaries appears fenestrated (wavy arrow).

(Group III, TEM × 4000).

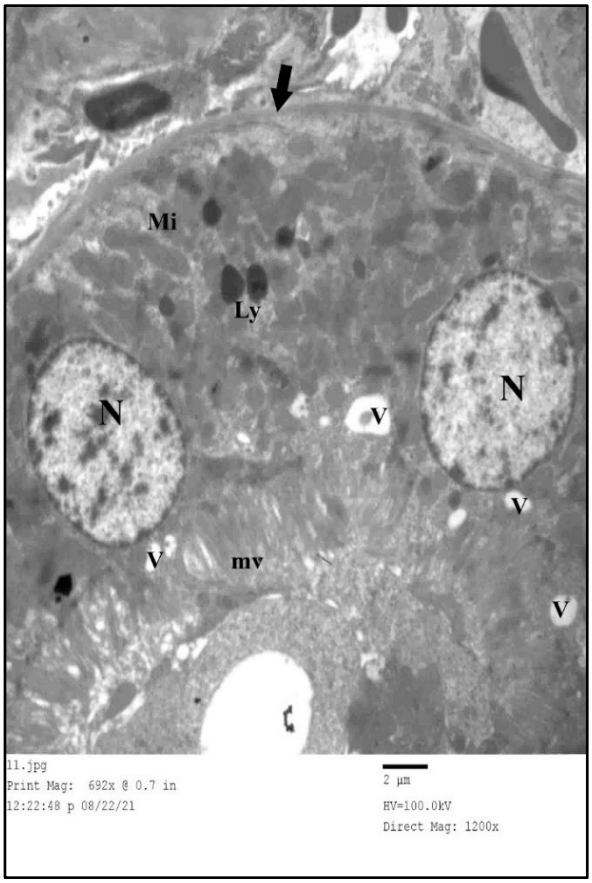

Figure 16:

TEM image of the renal cortex from **group III (treated group),** showing part of a PCT with an euchromatic rounded nucleus (N), elongated basal mitochondria (Mi) and basal infoldings. Notice: lysosomes (Ly) and endocytotic vesicles (V) in the apical cytoplasm are evident, and luminal border microvilli (mv) and thin basement membrane (short arrow) are seen.

(Group III, TEM × 1200)

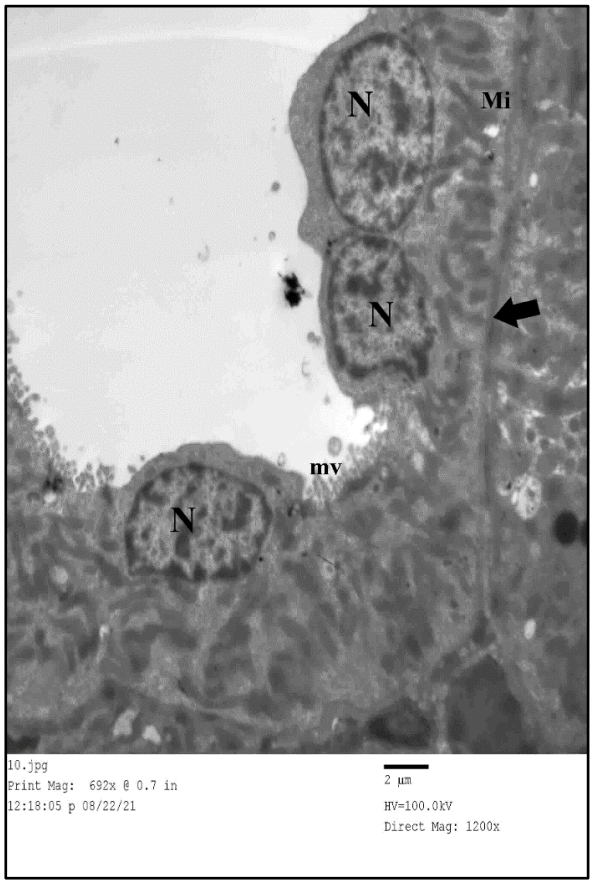

Figure 17:

TEM image of the renal cortex from **group III (treated group),** showing part of a DCT with oval euchromatic nuclei (N) and nearly normal basal infoldings with elongated basal mitochondria (Mi). Notice, few short microvilli (mv) and thin basement membrane (short arrow) are seen.

(Group III, TEM × 1200).

Statistical results:

Statistical comparison between control subgroups (Ia, Ib, and Ic) revealed nonsignificant changes ($p>0.05$).

1. The mean FBG levels were significantly greater in group II (diabetic) as compared to the other two groups ($p \leq 0.05$). Group III (treated) showed a significant decrease in FBG as compared to diabetic group, and a significant increase compared to group I ($p \leq 0.05$) Table (1) & Histogram (1).

Table 1: The mean FBG levels in the different groups.

Groups	Fasting Blood glucose (FBG) (mg/dl)
Group I	102.8 ± 3.7
Group II	440.4 ± 7.4▲
Group III	157 ± 5.56○■

▲Significant increase compared to all other groups
○Significant decrease compared to group II.
■Significant increase compared to group I.
p-values were calculated using analysis of variance (ANOVA).

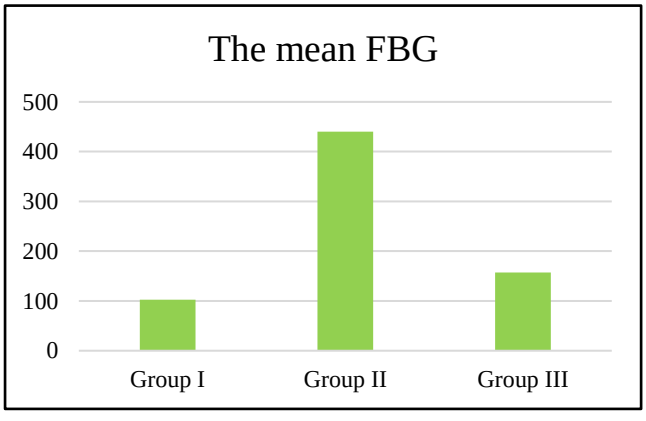

Histogram 1: The mean FBG levels in the different groups.

2. The mean area percentage (%) of collagen fibers was significantly greater in group II as compared to other groups. Moreover, treated group showed a significant decrease compared to diabetic group and a nonsignificant increase compared to group I Table (2) & Histogram (2).

Table 2: The mean area percentage (%) of collagen fibers in the different groups.

Groups	Area percentage (%) of collagen fibers
Group I	0.72±0.79
Group II	4.30±1.03▲
Group III	1.13±0.33○■

▲Significant increase compared to all other groups
○Significant decrease compared to group II.
■ Nonsignificant increase compared to control group I.
p-values were calculated using analysis of variance (ANOVA).

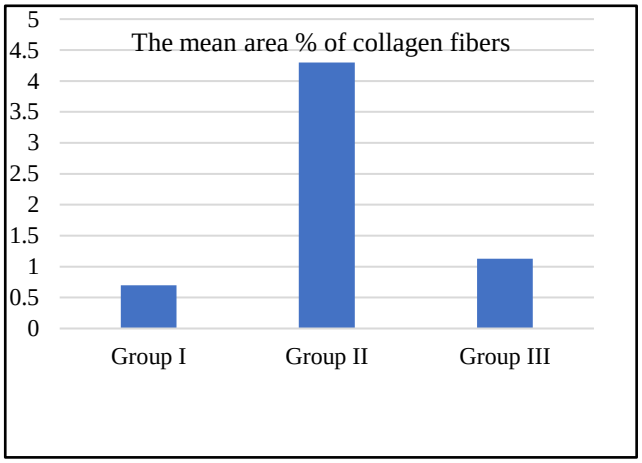

Histogram 2: The mean area percentage (%) of collagen fibers in the different group

3. The width (µm) of Bowman's space was significantly greater in diabetic group II as compared to other groups. Moreover, treated group showed a significant decrease as compared to the diabetic group and a nonsignificant increase as compared to group I Table (3) & Histogram (3).

Table 3: The width (µm) of Bowman's space in the different groups.

Groups	The width (µm) of Bowman's space
Group I	7.24±0.46
Group II	16.69±2.85▲
Group III	8.31±1.55 ○■

▲Significant increase compared to all other groups
○Significant decrease compared to group II.
■ Nonsignificant increase compared to control group I.
p-values were calculated using analysis of variance (ANOVA).

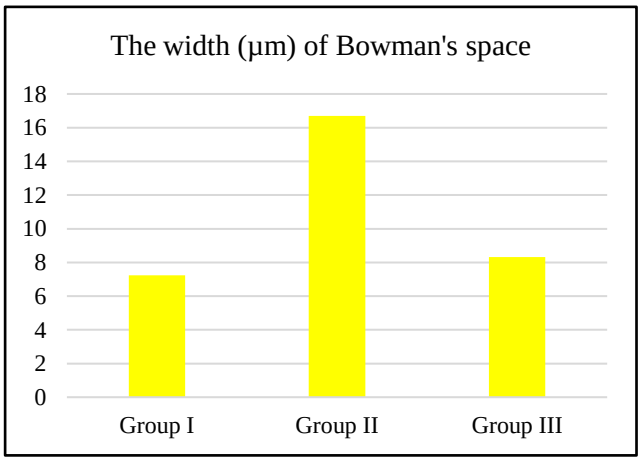

Histogram 3: The width (µm) of Bowman's space in the different

DISCUSSION:

In the current work, streptozotocin was used to induce DN in rats. LM examination of the kidney sections of group II (diabetic) animals revealed shrunken glomeruli with apparent dilatation of the capsular spaces of some renal corpuscles. This agreed with the findings of *Ebrahim et al.* [29] in albino rats with streptozotocin-induced diabetic nephropathy, which showed shrunken glomeruli and widened Bowman's spaces. There were two reasons for this shrinkage suggested by *Löwen et al.* [30], the first reason was the presence of glomerular vascular

defect characterized by increased leakiness, the second reason was increased production of glomerular basement membrane (GBM) components by podocytes and endothelial cells, resulting in the accumulation of GBM material in the mesangium. Glomerular degeneration could be induced by either defect. A shrunken tuft that fuses with Bowman's capsule to cause glomerular sclerosis would be the consequence of the progressive compaction of accumulated worn-out GBM material, as well as the retraction of podocytes out of the tuft and the collapse of capillaries [30].

The current study reported renal tubule dilatations, primarily in PCTs. According to a previous study, diabetes, which specifically causes proliferation in the proximal tubules of the kidney, is the cause of this tubular dilatation. Early proliferation of proximal tubules in diabetes patients is facilitated by a variety of growth factors, as platelet-derived growth factor, insulin-like growth factor 1, epidermal growth factor, and vascular endothelial growth factor [31]. Tubular dilatation, with or without protein casts, is a characteristic of tubular atrophy [32]. Additionally, tubular epithelial cells are less likely to receive oxygen and nutrients as a result of the intrarenal vasoconstriction linked to acute kidney injury, which causes the cells to flatten and atrophy [33].

Furthermore, the present investigation demonstrated that diabetes induces degenerative alterations in tubular cells, manifesting as deep acidophilic cytoplasm in certain cells and cytoplasmic vacuolization in others. Pyknotic nuclei were also present in conjunction with this. These findings were consistent with the findings of *Kengkoom et al.* [34] regarding streptozotocin-induced alpha-2u globulin nephropathy in rats. According to *Lau et al.* [35], cell adaptation to stressful conditions (hyperglycemia) and subsequent cell damage are the causes of tubule cell vacuolization. It is connected to subnuclear lipid vacuolization or glycogen deposition. They added that severe hyperglycemia can result in the formation of Armanni-Ebstein cells, which are tubule cells characterized by glycogen deposition. A previous study attributed this degeneration to oxidative stress (OS) which is accelerated by advanced glycation end products in DN. OS promotes the oxidative conversion of low-density lipoprotein (LDL) in the artery wall to oxidized LDL (ox-LDL), which is the initiating step in atherosclerosis development [32]. Even so, there is consistent evidence that the progression of chronic kidney disease (CKD) is progressively accelerated by ox-LDL, (a marker of oxidative stress), endothelial dysfunction (ED), and atherosclerosis [36]. To reduce nitric oxide (NO) bioavailability, which is required for vascular relaxation, OS promotes buildup of free radicals as DN worsens. Thus, LDL particles in the arterial wall are subjected to oxidative modification to produce ox-LDL, that in turn produces malondialdehyde (MDA), a lipid peroxide that is extremely reactive [36]. Then, MDA causes inflammatory cytokines and macrophages to adhere to ox-LDL particles, resulting in the formation of foam cells. By activating ox-LDL, OS causes ED, which is a defining feature of atherosclerosis in patients with CKD, moreover, hyperglycemic environment combined with ox-LDL leads to an excess of asymmetric dimethylarginine that encourages endothelial nitric oxide synthase uncoupling to form ROS [37]. Different research has demonstrated that ox-LDL determine ED in CKD patients [38]. According to earlier study [30], ox-LDL is a major factor in the development of glomerulosclerosis in diabetic kidney disease. Excessive ox-LDL uptake in renal tubular, renal epithelial, and mesangial cells has been noticed in experimental uremia and hyperglycemia; this results in intrarenal accumulation of lipid peroxides and loss of nephron [39]. According to *Gutwein et al.* [40], diabetic glomerulopathy is the result of oxidative modifications of

renal cells, which cause changes in their structure and function.

Thickened basement membrane was observed in some renal tubules in the present study in group II (diabetic). Some authors reported that the accumulation of glycoproteins resulting from renal damage and the upregulation of integrin, laminin and fibronectin causes thickening of basement membrane [41].

In group II (diabetic), the renal interstitium revealed infiltration of mono-nuclear inflammatory cells. This agreed with the findings of *Wellen & Hotamisligil* [42], who reported that oxidative stress induced by hyperglycemia increases proinflammatory protein levels by invading macrophages, which release inflammatory cytokines leading to tissue inflammation. According to a previous study, necrosis-induced tubular cell death can involve leukocytes and macrophages, among other inflammatory cells [43]. Furthermore, *Schelling* [32] linked blood infiltration and extravasation to atrophic tubules, which release pro-fibrotic and inflammatory cytokines.

Moreover, the accumulation of hyaline casts, an acidophilic substance, was commonly observed inside the tubule lumina of those that were impacted. A group of urine particles, as cells, fat, or microorganisms, attached to each other by a protein matrix, is known as a hyaline cast. The precipitation of the Tamm-Horsfall protein, which is secreted by epithelial tubule cells, is the cause. Hyaline casts are a sign of reduced urine flow, and a high concentration of these casts could reflect kidney damage as a result of reduced kidney blood flow [44].

In the present study, the sections of diabetic animals revealed increased collagen fibers in the kidney interstitium. This finding was in agreement with that of *Liu and Gaston pravia* [45], who reported that an increase in TGF-β due to increased oxidative stress promoted fibrosis in the interstitium. Previously, *Ziyadeh et al.* [46] reported that TGF-β expression increased in tubular epithelial cells, glomerular mesangial cells, and interstitial fibroblasts in hyperglycemic culture.

The present investigation revealed focal areas of lost brush border in cells lining some PCTs and disruption of the tubular basement membrane in PAS-stained kidney sections from group II (diabetic animals). This was in line with *Elsaed and Mohamed's* [47] theory which linked the loss to elevated free radical generation and decreased antioxidant synthesis, leading to an increase in tissue oxidative damage. Additionally, high glucose is linked to mesangial proliferation in diabetes by inducing hypertrophy and proliferation of mesangial cells simultaneously with TGF-β production. The hypertrophic effect of high glucose is inhibited in mesangial cells by neutralizing TGF-β antibody. In diabetic nephropathy, mesangial cell hypertrophy is largely caused by TGF-β signaling [48]. The subclassification of mesangial hypercellularity in each glomerulus is as follows: in terms of mesangial cells/mesangial area, fewer than four cells indicate normal cellularity, four to five cells indicate mild mesangial hypercellularity, six to seven cells indicate moderate mesangial hypercellularity, and eight or more cells/mesangial area indicate severe mesangial hypercellularity [49].

Transmission electron microscopy revealed that there was fusion of the podocyte foot processes as well as relative thickening of the glomerular basement membrane in diabetic rats. *Duni et al.* [50] linked podocyte injury to oxidative stress, which directly harms mesangial, endothelial, and podocytes. Reactive oxygen species (ROS) are produced by hyperglycemia via the NADPH oxidase enzyme and cause podocytes to separate from the GBM. Podocytes undergo apoptosis when ROS are produced [51&52].

Transmission electron microscopy revealed disorganized mitochondria,

disrupted basal cell membrane infoldings, and thicker tubular basement membranes in group II (diabetic animals). This was ascribed to ROS that might cause irreversible harm to proteins, lipids, and mitochondrial DNA, leading to dysfunctional mitochondria with cellular death. A previous study linked the rise in gene expression and protein synthesis, including that of collagen IV, laminin, and fibronectin, to the thickening of the glomerular and tubular basement membranes [46].

On the other hand, concomitant administration of FDGL extract with diabetes in group III animals was found to exert a protective effect. Most of the renal glomeruli appeared normal. Scattered tubules appeared dilatated. Few tubules showed vacuolations in the cytoplasm of their lining cells. Neither extravasated blood nor mononuclear cellular infiltration was noticed in the renal interstitium. Additionally, thin collagen fibers were observed around the tubules. By EM, GBM and podocytes were found to have a normal appearance. The PCTs and DCTs were surrounded by a relatively thin basement membrane with basal infoldings and elongated basal mitochondria. Lysosomes were also seen in the of the tubular cells. This finding agrees with *Schrier's* [53] who reported the presence of electron-dense bodies that were most likely secondary lysosomes. Early in DN, PCT lipofuscin pigments greatly increase; a high tubular lysosomal load may cause lipofuscin storage in DN [52]. Additionally, apical vacuoles in PCT-lining cells may be endocytotic vesicles of reabsorbed materials. The primary location of sugar reabsorption is the PCT; as sugar levels rise, so do these vesicles [53].

Yokozawa et al. [54] reported that liquorice extract reduced kidney damage by decreasing oxidative stress. Liquorice extract markedly attenuated kidney injury in diabetic rats due to its antioxidant effect [55].

Liquorice extract had significant antihyperglycemic activity. Liquorice provides protection by reducing oxidative stress caused by the production of free radicals induced by hyperglycemia [13]. *Baltina* [55] reported that after administering liquorice extract to diabetic rats for 60 days, the damage to the tubules and glomerulus was significantly reduced. The observed antihyperglycemic effect aligns with findings of *Mae et al.* [56], who stated that feeding genetically diabetic mice liquorice extract via a diet of 0.1–0.3/100 g (approximately 100–300 mg/kg body/day) for four weeks reduced blood glucose levels. Moreover, liquorice extract prevents and treats DN by blocking the activation of TGFβ signaling and Akt, also referred to as Protein Kinase B [57]. In another study, it was discovered that by inhibiting the notch2 signaling pathway, liquorice extract and deglycyrrhizinated liquorice extract reduce renal tubular epithelial-mesenchymal transition and fibrosis [58].

Liquorice extracts exhibit strong in vitro and in vivo antidiabetic properties. This can be explained by several mechanisms, including improving the body's microcirculation, removing free radicals and preventing peroxidation, boosting the sensitivity of the insulin receptor site to insulin, and improving the body's utilization of glucose in various tissues and organs [59].

According to *Yang et al.* [60], the primary active flavonoids of licorice that have anti-inflammatory properties are chalcones, which include licochalcone A and B, isoliquiritigenin, isoflavones, which include isoangustones A, and isoflavans, which include glabridin and licoricidin. Licochalcones A and B may downregulate prostaglandin E2, IL-6, and NO levels in lipopolysaccharides (LPS)-stimulated macrophages and suppress the production of ROS induced by LPS in macrophages in a dose-dependent manner [61]. Furthermore, by considerably decreasing the infiltration of the

white adipose tissue of the epididymis by inflammatory cells, isoliquiritigenin significantly reduced the inflammation caused by a high-fat diet in a mouse model [(62)]. In addition, by suppressing NO production induced by LPS and the expression of the inducible nitric oxide synthase (iNOS) gene in high-glucose environments, glabridin showed an anti-inflammatory effect on diabetes-related vascular dysfunction [(63)].

Furthermore, the anti-inflammatory characters of isoliquiritigenin are achieved by suppression of NF-κB activity, which causes a reduction in proinflammatory factors like TNF-α, IL-6, IL-1β, and IL-8 [(64)]. According to a different study, isoliquiritigenin may inhibit nuclear factor kappa B kinase, p38 phosphorylation, and extracellular signal-regulated kinase 1/2 (ERK1/2) in RAW 264.7 cells, which in turn may inhibit NF-κB and downstream iNOS, TNF-α, COX-2, and IL-6 [(65)]. According to *Li et al. B.* [(66)], isoliquiritigenin inhibited the downstream SMAD signaling pathway and inactivated the TGF-β RI and RII, thereby blocking mesangial proliferation and matrix deposition during DN. Isolequiritigenin also reduces the effects of STZ-induced diabetes by reducing inflammation, oxidative stress, and ED; it also downregulates miR-195, restoring retinal SIRT-1 levels, and tissue structure [(67)]. According to *Hasani-Ranjbar et al.* [(68)], polyphenols removed from Glycyrrhiza also decrease the serum levels of very-LDL-C, triglycerides, total cholesterol, and LDL cholesterol (LDL-C) by indirectly lowering LDL oxidation and eliminating free radicals as well as directly suppressing cholesterol biosynthesis. Additionally, *Fu et al.* [(61)] reported that licochalcone B and licochalcone A significantly reduced lipid peroxidation in rat liver microsomes and inhibited the production of ROS in RAW 264.7 cells caused by LPS.

It was previously proved that serum amylase and lipase were insufficient in patients with diabetic [(69)]. Fermentation of liquorice leads to the production of many essential enzymes such as amylase and lipase [(19)]. Hence the ameliorating effects of FDGL extract on the renal cortex of diabetic rats could be enhanced via the upsurge of the glycolytic enzymes' stores (due to fermentation), leading to improved diabetic management.

Conclusion and Recommendations:

FDGL extract substantially ameliorated the adverse effects of DM on the histological structure of renal cortex in diabetic rats. However, a variety of questions remain open. So further investigations are recommended to evaluate the therapeutic as well as the protective potential of FDGL extract against the deleterious effects of DM on different tissues and organs.

List of abbreviations:

µm	: micrometer
CKD	: chronic kidney disease
DCTs	: distal convoluted tubules
DM	: Diabetes Mellitus
DN	: Diabetic nephropathy
ED	: endothelial dysfunction
EM	: electron microscopy
FDGL	: fermented deglycyrrhizinated liquorice extract.
GBM	: glomerular basement membrane
H&E	: hematoxylin and eosin
LDL	: low-density lipoprotein
LM	: light microscopy
NO	: nitric oxide
ox-LDL	: oxidized LDL
PAS	: periodic acid Schiff
PCTs	: proximal convoluted tubules
STZ	: streptozotocin.
TEM	: transmission electron microscopy

REFERENCES:

1. **Valencia W. M., Florez H (2017):** How to prevent the microvascular complications of type 2 diabetes beyond glucose control. BMJ. 356, article i6505.
2. **Xue R., Gui D., Zheng L., Zhai R., Wang F., Wang N (2017):** Mechanistic insight and management of diabetic nephropathy: recent progress and future perspective. Journal of Diabetes Research. 2017:7.

3. **Tavafi M (2013):** Diabetic nephropathy and antioxidants. Journal of Nephropathology. 2:20–27.
4. **Donate-Correa J., Luis-Rodríguez D., Martín-Núñez E., et al (2020):** Inflammatory targets in diabetic nephropathy. Journal of Clinical Medicine. ;9 (2): 458.
5. **Kao MP, Ang DS, Pall A, Struthers AD.** Oxidative stress in renal dysfunction: mechanisms, clinical sequelae and therapeutic options. J Hum Hypertens. 2010 Jan;24(1):1-8. doi: 10.1038/jhh.2009.70. PMID: 19727125.
6. **Kopel J., Pena-Hernandez C., Nugent K (2019):** Evolving spectrum of diabetic nephropathy. World Journal of Diabetes. 10:269–279.
7. **Shang J, Wang L, Zhang Y, Zhang S, Ning L, Zhao J, Cheng G, Liu D, Xiao J, Zhao Z.** Chemerin/ChemR23 axis promotes inflammation of glomerular endothelial cells in diabetic nephropathy. J Cell Mol Med. 2019 May;23(5):3417-3428. doi: 10.1111/jcmm.14237. Epub 2019 Feb 19. PMID: 30784180; PMCID: PMC6484295.
8. **Zhao Y, Lv B, Feng X, Li C.** Perspective on Biotransformation and De Novo Biosynthesis of Licorice Constituents. J Agric Food Chem. 2017 Dec 27;65(51):11147-11156. doi: 10.1021/acs.jafc.7b04470. Epub 2017 Dec 13. PMID: 29179542.
9. **Cheng M, Zhang J, Yang L, Shen S, Li P, Yao S, Qu H, Li J, Yao C, Wei W, Guo DA.** Recent advances in chemical analysis of licorice (Gan-Cao). Fitoterapia. 2021 Mar;149:104803. doi: 10.1016/j.fitote. 2020.104803. Epub 2020 Dec 10. PMID: 33309652.
10. **Yang L, Jiang Y, Zhang Z, Hou J, Tian S, Liu Y**. The anti-diabetic activity of licorice, a widely used Chinese herb. J Ethnopharmacol. 2020 Dec 5;263:113216. doi: 10.1016/j.jep.2020.113216. Epub 2020 Aug 5. PMID: 32763420.
11. **Nakagawa K, Kishida H, Arai N, Nishiyama T, Mae T.** Licorice flavonoids suppress abdominal fat accumulation and increase in blood glucose level in obese diabetic KK-A(y) mice. Biol Pharm Bull. 2004 Nov;27(11):1775-8. doi: 10.1248/bpb.27.1775. PMID: 15516721.
12. **Yoshioka Y, Yamashita Y, Kishida H, Nakagawa K, Ashida H.** Licorice flavonoid oil enhances muscle mass in KK-A^y mice. Life Sci. 2018 Jul 15;205:91-96. doi: 10.1016/j.lfs.2018.05.024. Epub 2018 May 16. PMID: 29753766.
13. **Shibata S. (2000).** A drug over the millennia: pharmacognosy, chemistry, and pharmacology of liquorice. Yakugaku Zasshi 120:849–862.
14. **Wang, Z. Y., Nixon, D. W. (2001):** Liquorice and cancer. Nutr Cancer 39:1–11.
15. **Nakagawa T, Yokozawa T, Kim YA, Kang KS, Tanaka T.** Activity of wen-pi-tang, and purified constituents of rhei rhizoma and glycyrrhizae radix against glucose-mediated protein damage. Am J Chin Med. 2005;33(5):817-29. doi: 10.1142/S0192415 X05003375. PMID: 16265994.
16. **Weidner, C., De Groot, J. C., Prasad, A., Freiwald, A., Quedenau, C., Kliem, M., et al. (2012):** Amorfrutins are potent antidiabetic dietary natural products. Proc. Natl. Acad. Sci. U.S.A. 109, 7257–7262.
17. **Yang, R., et al. (2015):** The pharmacological activities of liquorice. Planta Medica, 81(18), 1654–1669.
18. **Giulia P, Laura C, Sónia S, Francisca R, Beatriz P (2018):** Liquorice (Glycyrrhiza glabra): A phytochemical and pharmacological review. Phytother Res 32: 2323- 2339.
19. **Massoud AMA (2011):** Global Patent Index - EP 1925312 B1.
20. **Noreen S, Mubarik F, Farooq F, Khan M, Khan AU, Pane YS (2021):** Medicinal Uses of Liquorice (Glycyrrhiza glabra L.): A Comprehensive Review. Open-Access Maced J Med Sci. 27; 9(F): 668-675.
21. **Sawada K, Yamashita Y, Zhang T, Nakagawa K, Ashida H (2014):** Glabridin induces glucose uptake via the AMP-activated protein kinase pathway in muscle cells. Molecular and Cellular Endocrinology. Volume 393, Issues 1– 2, 5, Pages 99-108.

22. **Buck WB, Osweiter GD, Van GA (1976):** Clinical and diagnostic veterinary toxicology. Kendall/Hunt Publishing Company 52011.

23. **Afifi N, Ramadan A, El-Aziz MI, Saki E (1991):** Influence of dimethoate on testicular and epididymal organs, testosterone plasma level and their tissue residues in rats. Dtsch Tierarztl Wochenschr 98: 419-423.

24. **Zangiabadi N, Sheibani V, Asadi-Shekaari M, Shabani M, Jafari M, et al. (2011):** Effects of Melatonin in Prevention of Neuropathy in STZ-Induced Diabetic Rats. American Journal of Pharmacology and Toxicology 6: 59-67.

25. **El-Waseef DA** and **Abd Al-Khalek HA.** Effect of Bee Venom on the Structure of unwounded thick Skin in Adult Male Diabetic Rats: Histological, Immunohistochemical and Morphometric Study. J Am Sci 2017;13(1):159-166]. ISSN 1545-1003 (print); ISSN 2375-7264 (online). http://www.jofamericanscience.org. 22. doi:10.7537/marsjas130117.22.

26. **Amaral S, Santos MS, Seica R, Ramalho SJ, Moreno AJ (2006):** Effects of hyperglycemia on sperm and testicular cells of Goto-Kakizaki and streptozotocin-treated rat models for diabetes. Theriogenology 66: 2056-2067.

27. **Massoud AMA, Ebiary FHE, Raafat MH, Hamam GG, Mostafa HKK (2019):** The Effect of Fermented Deglycyrrhizinized Liquorice Extract on the Structure of Gastrocnemius Muscle and Sciatic Nerve in Experimentally Induced Diabetes Mellitus in Rats: Histopathological Study. J Cytol Histol 10: 544.

28. **Suvarna KS, Layton C, and Bancroft JD (2013):** Theory and practice of histological techniques. (7th edtn), USA: Churchill Livingston.

29. **Ebrahim R, Mostafa O and Mohamed E (2019):** Effect of Low and High Doses of Vitamin D on Streptozotocin Induced Diabetic Nephropathy in Adult Male Albino Rats: Histological and Immunohistochemical Study. Vol. 42, No.

30. **Löwen J , Gröne EF, Groß-Weißmann ML, Bestvater F, Gröne HJ , Kriz W (2021):** Pathomorphological sequence of nephron loss in diabetic nephropathy. Am J Physiol Renal Physiol. 1;321(5): F600-F616.

31. **Vallon V, Thomson SC (2012):** Renal function in diabetic disease models: the tubular system in the pathophysiology of the diabetic kidney. Annu Rev Physiol; 74: 351-75.

32. **Schelling J. R. (2016).** Tubular atrophy in the pathogenesis of chronic kidney disease progression. *Pediatric nephrology (Berlin, Germany)*, *31*(5), 693–706. https://doi.org/10.1007/s00467-015-3169-4

33. **Kumar V, Abbas AK and Aster JC (2013):** Robbins basic pathology. W.B. Saunders El Sevier Inc, 9th edition; 537- 538 and p 21.

34. **Kengkoom K, Angkhasirisap W, Kanjanapruthipong T, Tuentam K, Phansom N&Ampawong S (2021):** Streptozotocin induces alpha-2u globulin nephropathy in male rats during diabetic kidney disease. BMC Veterinary Research volume 17, Article number: 105.

35. **Lau X, Zhang Y, Kelly DJ, Stapleton DI (2013):** Attenuation of Armanni–Ebstein lesions in a rat model of diabetes by a new anti-fibrotic, anti-inflammatory agent, FT011. Diabetologia,56:675–679.

36. **Roumeliotis S, Roumeliotis A, Gorny X, Mertens PR.** Could Antioxidant Supplementation Delay Progression of Cardiovascular Disease in End-Stage Renal Disease Patients? Curr Vasc Pharmacol. 2021;19(1):41-54. doi: 10.2174/1570161118666200317151553. PMID: 32183680.

37. **Roumeliotis S, Mallamaci F, Zoccali C.** Endothelial Dysfunction in Chronic Kidney Disease, from Biology to Clinical Outcomes: A 2020 Update. J Clin Med. 2020 Jul 23;9(8):2359. doi: 10.3390/jcm9082359. PMID: 32718053; PMCID: PMC7465707.

38. **Nawrot TS, Staessen JA, Holvoet P, Struijker-Boudier HA, Schiffers P, Van Bortel LM, Fagard RH, Gardner JP, Kimura M, Aviv A.** Telomere length and its associations with oxidized-LDL, carotid artery distensibility and smoking. Front

Biosci (Elite Ed). 2010 Jun 1;2(3):1164-8. doi: 10.2741/e176. PMID: 20515788.

39. **Nosadini R, Tonolo G.** Role of oxidized low-density lipoproteins and free fatty acids in the pathogenesis of glomerulopathy and tubulointerstitial lesions in type 2 diabetes. Nutr Metab Cardiovasc Dis. 2011 Feb;21(2):79-85. doi: 10.1016/j.numecd .2010.10.002. Epub 2010 Dec 24. PMID: 21186102.
40. **Gutwein, P., Abdel-Bakky, M.S., Doberstein, K., Schramme, A., Beckmann, J., Schaefer, L., Amann, K., Doller, A., Kämpfer-Kolb, N., Abdel-Aziz, A.-A.H., Sayed, E.S.M.E. and Pfeilschifter, J. (2009):** CXCL16 and oxLDL are induced in the onset of diabetic nephropathy. Journal of Cellular and Molecular Medicine, 13: 3809-3825. https://doi.org/10.1111/j.1582-4934.2009.00761.x.
41. **Ghaly EN, Gergis SW, Aziz JN, Yassa HD, Hassan HA (2014):** Role of mesenchymal stem cell therapy in cisplatin induced nephrotoxicity in adult albino rats: ultrastructural and biochemical study. Acta Medica international, 32(1): 57- 66.
42. **Wellen KE, Hotamisligil GS (2005):** Inflammation, stress, and diabetes. J Clin Invest. ;115(5):1111-1119.
43. **Chang B, Nishikawa M, Sato E, Utsumi K, Inouea ML (2002):** Carnitine inhibits cisplatin-induced injury of the kidney and small intestine. Archives of Biochemistry and Biophysics 2002; 405: 55- 64.
44. **Cavanaugh C, Perazella MA (2019):** Urine sediment examination in the diagnosis and management kidney disease: Core curriculum 2019. Am J Kidney Dis; 73: 258-272.
45. **Liu RM, Gaston Pravia KA**. Oxidative stress and glutathione in TGF-beta-mediated fibrogenesis. Free Radic Biol Med. 2010 Jan 1;48(1):1-15. doi: 10.1016/j.freeradbiomed. 2009.09.026. Epub 2009 Oct 2. PMID: 19800967; PMCID: PMC2818240.
46. **Ziyadeh FN, Hoffman BB, Han DC, et al (2000):** Long-term prevention of renal insufficiency, excess matrix gene expression, and glomerular mesangial matrix expansion by treatment with monoclonal antitransforming growth factor-β antibody in db/db diabetic mice. Proc Natl Acad Sci U S A; 97: 8015-20.
47. **Elsaed WM, Mohamed HA.** Dietary zinc modifies diabetic-induced renal pathology in rats. Ren Fail. 2017 Nov;39(1):246-257. doi: 10.1080/0886022X.2016.1256321. Epub 2016 Nov 24. PMID: 27882813; PMCID: PMC6014501.
48. **Mahimainathan L, Das F, Venkatesan B, Choudhury GG**. Mesangial cell hypertrophy by high glucose is mediated by downregulation of the tumor suppressor PTEN. Diabetes. 2006 Jul;55(7):2115-25. doi: 10.2337/db05-1326. PMID: 16804083.
49. **Roberts, I. S., Cook, H. T., Troyanov, S., Alpers, C. E., Amore, A., Barratt, J., Berthoux, F., Bonsib, S., Bruijn, J. A., Cattran, D. C., Coppo, R., D'Agati, V., D'Amico, G., Emancipator, S., Emma, F., Feehally, J., Ferrario, F., Fervenza, F. C., Florquin, S., Zhang, H. (2009).** The Oxford classification of IgA nephropathy: pathology definitions, correlations, and reproducibility. *Kidney international*, *76*(5), 546–556. https://doi.org/10.1038/ki.2009.168Jia
50. **Duni A., Liakopoulos V., Roumeliotis S., Peschos D., Dounousi E (2019):** Oxidative stress in the pathogenesis and evolution of chronic kidney disease: untangling Ariadne's thread. International Journal of Molecular Sciences. 20: p. 3711.
51. **Jia J, Ding G, Zhu J, Chen C, Liang W, Franki N, Singhal PC.** Angiotensin II infusion induces nephrin expression changes and podocyte apoptosis. Am J Nephrol. 2008;28(3):500-7. doi: 10.1159/000113538. Epub 2008 Jan 17. PMID: 18204248; PMCID: PMC2630486.
52. **Pourghasem M, Shafi H, Babazadeh Z (2015):** Histological changes of kidney in diabetic nephropathy Caspian J Intern Med; 6(3):120-127.
53. **Schrier, R.W. (2006):** Diseases of the kidney and urinary tract. 8th ed. P.2159-2178. Lippincott Williams and Wilkins.
54. **Yokozawa, T., Cho, E. J., Rhyu, D. Y., Shibahara, N., Aoyagi, K. (2005):** Glycyrrhizae radix attenuates peroxynitrite-

induced renal oxidative damage through inhibition of protein nitration. Free Radic Res 39:203–211.

55. **Baltina, L. A. (2003):** Chemical modification of glycyrrhizic acid as a route to new bioactive compounds for medicine. Curr Med Chem 10:155–171.
56. **Mae T, Kishida H, Nishiyama T, Tsukagawa M, Konishi E, Kuroda M, Mimaki Y, Sashida Y, Takahashi K, Kawada T, Nakagawa K, Kitahara M.** A licorice ethanolic extract with peroxisome proliferator-activated receptor-gamma ligand-binding activity affects diabetes in KK-Ay mice, abdominal obesity in diet-induced obese C57BL mice and hypertension in spontaneously hypertensive rats. J Nutr. 2003 Nov;133(11):3369-77. doi: 10.1093/jn/133.11.3369. PMID: 14608046.
57. **Li J, Lee YS, Choi JS, Sung HY, Kim JK, Lim SS, Kang YH (2010)-A:** Liquorice extracts dampen high glucose-induced mesangial hyperplasia and matrix deposition through blocking Akt activation and TGF-beta signaling. Phytomedicine. 17:800–810.
58. **Hsu YC, Chang PJ, Tung CW, Shih YH, Ni WC, Li YC, Uto T, Shoyama Y, Ho C, Lin CL (2020):** De-Glycyrrhizinated Liquorice Extract Attenuates High Glucose-Stimulated Renal Tubular Epithelial-Mesenchymal Transition via Suppressing the Notch2 Signaling Pathway. Cells. 5;9(1):125.
59. **Yang L, Jiang Y, Zhang Z, Hou J, Tian S, Liu Y (2020):** The anti-diabetic activity of liquorice, a widely used Chinese herb..J Ethnopharmacol. 5; 263:113216.
60. **Yang R, Yuan BC, Ma YS, Zhou S, Liu Y.** The anti-inflammatory activity of licorice, a widely used Chinese herb. Pharm Biol. 2017 Dec;55(1):5-18. doi: 10.1080/13880209. 2016.1225775. Epub 2016 Sep 21. PMID: 27650551; PMCID: PMC7012004.
61. **Fu Y, Chen J, Li YJ, Zheng YF, Li P.** Antioxidant and anti-inflammatory activities of six flavonoids separated from licorice. Food Chem. 2013 Nov 15;141(2):1063-71. doi: 10.1016/j.foodchem.2013.03.089. Epub 2013 Apr 13. PMID: 23790887.
62. **Honda H, Nagai Y, Matsunaga T (2014):** Isoliquiritigenin is a potent inhibitor of NLRP3 inflammasome activation and diet-induced adipose tissue inflammation, Journal of Leukocyte Biology, vol. 96, no. 6, pp. 1087–1100.
63. **Yehuda I, Madar Z, Leikin-Frenkel A, Tamir S (2015):** Glabridin, an isoflavan from licorice root, downregulates iNOS expression and activity under high-glucose stress and inflammation, Molecular Nutrition & Food Research, vol. 59, no. 6, pp. 1041–1052.
64. **Liao Y, Tan RZ, Li JC, Liu TT, Zhong X, Yan Y, Yang JK, Lin X, Fan JM, Wang L.** Isoliquiritigenin Attenuates UUO-Induced Renal Inflammation and Fibrosis by Inhibiting Mincle/Syk/NF-Kappa B Signaling Pathway. Drug Des Devel Ther. 2020 Apr 14;14:1455-1468. doi: 10.2147/DDDT.S243420. PMID: 32341639; PMCID: PMC7166058.
65. **Kim JY, Park SJ, Yun KJ, Cho YW, Park HJ, Lee KT (2008):** Isoliquiritigenin isolated from the roots of Glycyrrhiza uralensis inhibits LPS-induced iNOS and COX-2 expression via the attenuation of NF-kappaB in RAW 264.7 macrophages. Eur J Pharmacol. 2008 Apr 14;584(1):175-84. doi: 10.1016/j.ejphar.2008.01.032. Epub 2008 Feb 5. PMID: 18295200.
66. **Li J, Kang SW, Kim JL, Sung HY, Kwun IS, Kang YH (2010)-B:** Isoliquiritigenin entails blockade of TGF-beta1-SMAD signaling for retarding high glucose-induced mesangial matrix accumulation. J Agric Food Chem. 2010 Mar 10;58(5):3205-12. doi: 10.1021/jf9040723. PMID: 20146476
67. **Alzahrani S, Ajwah SM, Alsharif SY, Said E, El-Sherbiny M, Zaitone SA, Al-Shabrawey M, Elsherbiny NM.** Isoliquiritigenin downregulates miR-195 and attenuates oxidative stress and inflammation in STZ-induced retinal injury. Naunyn Schmiedebergs Arch Pharmacol. 2020 Dec;393(12):2375-2385. doi: 10.1007/ s00210-020-01948-5. Epub 2020 Jul 22. Retraction in: Naunyn Schmiedebergs Arch Pharmacol. 2023 Nov;396(11):3345. PMID: 32699958.

68. **Hasani-Ranjbar S, Nayebi N, Moradi L, Mehri A, Larijani B, Abdollahi M.** The efficacy and safety of herbal medicines used in the treatment of hyperlipidemia; a systematic review. Curr Pharm Des. 2010;16(26):2935-47. doi: 10.2174/138161 210793176464. PMID: 20858178.

69. **Aughsteen A, Abu UM, Mahmoud S (2005):** Biochemical analysis of 8. serum pancreatic amylase and lipase enzymes in patients with type 1 and 2 diabetes mellitus. Saudi Med J 26: 73-77.

تأثير مستخلص عرق السوس منزوع الجليسيرهيزين المخمر على تركيب القشرة الكلوية في داء السكري المستحث تجريبيا في الجرذان: دراسة نسيجية مرضية

أحمد محمد علي مسعود[1]، فائقة حسن الإبياري[2]، نيبال جمال عبد الوهاب[2]، داليا علاء الدين علي الوصيف[2]

قسم أمراض الكبد والجهاز الهضمي والأمراض المعدية - كلية الطب جامعة الأزهر- القاهرة - مصر[1]
قسم الأنسجة وبيولوجيا الخلية - كلية الطب جامعة عين شمس – القاهرة - مصر[2]

المقدمة: يعتبر اعتلال الكلية السكري أحد أخطر وأشد مضاعفات مرض السكري. تم تخمير العرق سوس وإزالة الجليسيرهيزين. ومن ثم، تم استخدام مصطلح مستخلص عرق السوس منزوع الجليسيرهيزين المخمر.

الهدف من البحث: دراسة التأثير التحسيني المحتمل لعرق السوس منزوع الجليسيرهيزين المخمر على بنية قشرة الكلى في الجرذان المصابة بداء السكري المستحث تجريبياً.

المواد والطرق المستخدمة: تم تقسيم خمسة وأربعين من ذكور الجرذان البيضاء البالغة إلى ثلاث مجموعات. المجموعة الأولى (المجموعة الضابطة)، المجموعة الثانية (مجموعة مرضى السكري): تم إحداث مرض السكري عن طريق حقن الستربتوزوتوسين والمجموعة الثالثة (المجموعة المصابة بالسكري والمعالجة بعرق السوس منزوع الجليسيرهيزين المخمر: تركت الفئران المصابة بداء السكري دون علاج لمدة أسبوعين ثم عولجت بعرق السوس منزوع الجليسيرهيزين المخمر (0.12 جم/كجم من وزن الجسم/اليوم عن طريق الفم) لمدة أسبوعين آخرين قبل التضحية بهم.

النتائج: أظهرت المجموعة الثانية بعض الكبيبات الكلوية المنكمشة مع اتساع مساحات بومان. بينما لوحظ تمدد الكبيبات الأخرى. ظهرت الأنابيب الملتوية القريبة متسعة مع وجود ترسبات. أظهر النسيج الخلالي دمًا متسربًا، و تجمع للخلايا أحادية النواة، وزيادة في ألياف الكولاجين، وفقدانًا بؤريًا للفرشاة القمية، و تمزق الغشاء القاعدي للأنابيب الملتوية القريبة. أظهر المجهر الإلكتروني التحام الزوائد القدمية للخلايا القدمية وزيادة سمك الغشاء القاعدي الكبيبي. كما أظهرت الأنابيب الملتوية القريبة فجوات السيتوبلازم والميتوكوندريا غير المنظمة. مقارنة بالمجموعة الثانية، أظهرت المجموعة الثالثة استعادة نسبية للبنية النسيجية الطبيعية للكبيبات والأنابيب الكلوية.

الاستنتاج: أظهرت نتائج الدراسة الحالية أن مستخلص عرق السوس منزوع الجليسيرهيزين المخمر خفف بشكل كبير من الآثار الضارة لمرض السكري على بنية القشرة الكلوية في الجرذان المصابة بالسكري.